



Published in final edited form as:

Am J Transplant. 2019 March ; 19(3): 884–893. doi:10.1111/ajt.15196.

Ablation of interferon regulatory factor 4 in T cells induces “memory” of transplant tolerance that is irreversible by immune checkpoint blockade

Hedong Zhang^{#1,2}, Jie Wu^{#1,3}, Dawei Zou¹, Xiang Xiao¹, Hui Yan¹, Xian C. Li^{1,4}, and Wenhao Chen^{1,4}

¹Immunobiology & Transplant Science Center, Houston Methodist Research Institute, Texas Medical Center, Houston, Texas

²Department of Urological Organ Transplantation, Center of Organ Transplantation, The Second Xiangya Hospital of Central South University, Changsha, China

³Department of Cardiovascular Surgery, Tongji Medical College, Huazhong University of Science and Technology, Union Hospital, Wuhan, China

⁴Department of Surgery, Weill Cornell Medical College, Cornell University, New York, New York

These authors contributed equally to this work.

Abstract

Achieving transplant tolerance remains the ultimate goal in the field of organ transplantation. We demonstrated previously that ablation of the transcription factor interferon regulatory factor 4 (IRF4) in T cells induced heart transplant acceptance by driving allogeneic CD4⁺ T cell dysfunction. Herein, we showed that heart-transplanted mice with T cell-specific IRF4 deletion were tolerant to donor-specific antigens and accepted the subsequently transplanted donor-type but not third-party skin allografts. Moreover, despite the rejection of the primary heart grafts in T cell-specific *Irf4* knockout mice under immune checkpoint blockade, the establishment of donor-specific tolerance in these mice was unhindered. By tracking alloantigen-specific CD4⁺ T cells in vivo, we revealed that checkpoint blockade restored the expression levels of the majority of wild-type T cell-expressed genes in *Irf4*-deficient T cells on day 6 post-heart grafting, indicating the initial reinvigoration of *Irf4*-deficient T cells. Nevertheless, checkpoint blockade did not restore cell frequency, effector memory cell generation, and IFN- γ /TNF- α production of *Irf4*^{-/-} alloreactive T cells at day 30 post-heart grafting. Hence, targeting IRF4 represents a potential therapeutic strategy for driving intrinsic T cell dysfunction and achieving alloantigen-specific transplant tolerance.

Correspondence Wenhao Chen wchen@houstonmethodist.org.

DISCLOSURE

The authors of this manuscript have no conflicts of interest to disclose as described by the *American Journal of Transplantation*.

SUPPORTING INFORMATION

Additional supporting information may be found online in the Supporting Information section at the end of the article.

Keywords

animal models; murine, basic (laboratory) research/science; cellular biology; graft survival; immunobiology; organ transplantation in general; T cell biology; tolerance

1 | INTRODUCTION

Organ transplantation is a life-saving treatment for patients with end-stage organ failure, but long-term graft survival is limited by immune rejection and side effects of immunosuppressive drugs.¹ Allogeneic T cell response plays a decisive role in transplant rejection. The activation signals through T cell receptor (TCR), along with costimulation and cytokine inputs, mediate T cell response to organ transplants.²⁻⁴ Hence, for more effective control of transplant immunity, it is essential to define the key regulators that link the TCR and other signals to the functional fates of alloreactive T cells.

Interferon regulatory factor 4 (IRF4) is a member of the IRF family of transcription factors. IRF4 is preferentially expressed in hematopoietic cells and plays critical roles in the differentiation and function of T cells, B cells and dendritic cells.⁵⁻⁷ We found that IRF4 was promptly induced in T cells upon TCR signaling through the MEK1/2 pathway. IRF4 ablation in T cells resulted in progressive establishment of CD4⁺ T cell dysfunction and induced heart allograft acceptance in mice. The dysfunctional state of *Irf4*^{-/-} T cells was initially reversible by blocking programmed death-ligand 1 (PD-L1) and cytotoxic T-lymphocyte-associated protein 4 (CTLA-4), but it progressively developed into a terminal/irreversible dysfunctional state.⁸ Therefore, the TCR-IRF4 axis governs the functional versus dysfunctional fates of alloreactive T cells.

Recent reports showed that in patients with stable function of transplanted kidneys but also developed metastatic cancer, programmed cell death protein 1 (PD-1) blockade was used to treat cancer. Unfortunately, PD-1 blockade triggered acute rejection of the transplanted kidneys.^{9,10} Therefore, irreversible dysfunction of alloreactive T cells was not established in those kidney recipients, though they were under chronic immunosuppression. Low dose of FK506, the mainstay immunosuppressant, has even been shown to inhibit the terminal differentiation of T cell dysfunction.¹¹ Hence, in the context of achieving stable transplant tolerance, it would be essential to define the irreversible state of T cell dysfunction.

Herein, we investigated the irreversible dysfunctional state of *Irf4*^{-/-} T cells. *Irf4*^{fl/fl}*Cd4*-Cre heart recipients were treated with checkpoint blockade on days 0, 3, and 5, and transplanted again with donor-type skin grafts on day 30 post-heart grafting. All heart allografts were acutely rejected due to checkpoint blockade-mediated reinvigoration of *Irf4*^{-/-} T cells.⁸ Strikingly, those *Irf4*^{fl/fl}*Cd4*-Cre recipients with rejected heart allografts still permanently accepted the subsequent donor-type skin grafts, indicating that checkpoint blockade-reinvigorated alloreactive *Irf4*^{-/-} T cells become re-dysfunction within 30 days. Indeed, initial checkpoint blockade did not restore cell frequency, effector memory cell generation, and IFN- γ /TNF- α production of alloreactive *Irf4*^{-/-} T cells at day 30 post-heart grafting. Taken together, ablation of IRF4 drives terminal T cell dysfunction, and targeting IRF4 represents a potential therapeutic strategy for achieving transplant tolerance.

2 | MATERIALS AND METHODS

2.1 | Mice

Cd4-Cre, *Irf4*^{fllox/fllox}, B6.SJL CD45.1 congenic, TEa TCR transgenic,⁸ BALB/c, and C57BL/6 (B6) mice were purchased from Jackson Laboratory (Bar Harbor, MA). *Irf4*^{fllox/fllox} mice were crossed to *Cd4*-Cre mice to create *Irf4*^{fl/fl}*Cd4*-Cre mice. TEa mice were crossed to *Irf4*^{-/-} mice to create *Irf4*^{-/-} TEa mice. TEa mice were crossed to CD45.1 congenic mice to create (TEa × CD45.1) F1 mice, in which leucocytes are CD45.1⁺CD45.2⁺. All animal experiments in this study were approved by the Houston Methodist Animal Care Committee in accordance with institutional animal care and use guidelines.

2.2 | Murine heterotopic heart transplantation

Hearts from BALB/c donors were transplanted into 8-10-week-old male *Irf4*^{fl/fl}*Cd4*-Cre or CD45.1⁺ congenic mice by a previously described method.⁸ Some recipient mice were ip injected with 400 µg Rat IgG, or 200 µg anti-PD-L1 (clone 10F.9G2) plus 200 µg anti-CTLA-4 (clone 9D9) mAbs (Bio-X-Cell, West Lebanon, NH) on days 0, 3, 5 post-heart grafting.

2.3 | Murine skin transplantation

BALB/c and C3H ear skin allografts were transplanted onto BALB/c heart transplanted *Irf4*^{fl/fl}*Cd4*-Cre mice by a previously described method.¹² More than 80% necrosis of the donor skin tissue was considered as rejection.

2.4 | *Irf4* transduction and adoptive transfer of *Irf4*^{-/-} CD4⁺ T cells

BALB/c splenic dendritic cells (DCs) were isolated by using the Pan Dendritic Cell Isolation Kit (Miltenyi Biotec, San Diego, CA). *Irf4*^{-/-} CD4⁺ T cells were activated for 3 days with BALB/c splenic DCs and 100 IU IL-2 (PeproTech, Rocky Hill, NJ), and then transduced with IRF4-GFP or GFP-Ctrl retrovirus as previously described.⁸ Cells were cultured for 1 day after transduction, and then adoptively transferred into *Irf4*^{fl/fl}*Cd4*-Cre mice on day 1 post-heart transplantation.

2.5 | Adoptive transfer of TEa cells and microarray analysis

Microarray was performed by the Genomic and RNA Profiling Core at Baylor College of Medicine and data generated has been deposited in NCBI's Gene Expression Omnibus with accession number GSE111757. TCR(Vα2⁺Vβ6⁺)CD45.2⁺CD4⁺ TEa cells were isolated from splenocytes of WT TEa or *Irf4*^{-/-} TEa mice by a FACSAria flow cytometer (BD Biosciences, San Jose, CA). B6.SJL CD45.1⁺ congenic mice were adoptively transferred with either 5 × 10⁶ CD45.2⁺ WT TEa or 5 × 10⁶ CD45.2⁺ *Irf4*^{-/-} TEa cells on day -1, and transplanted with BALB/c hearts on day 0. CD45.1⁺ mice transferred with CD45.2⁺ *Irf4*^{-/-} TEa cells were ip injected with either 400 µg Rat IgG or 200 µg anti-PD-L1 plus 200 µg anti-CTLA-4 mAbs on days 0, 3, 5. On day 6, adoptively transferred CD45.2⁺ TEa cells were sorted for microarray analysis, using a previously described method.⁸

2.6 | Tracking of adoptively transferred TEa cells

CD45.1⁺ congenic mice were adoptively transferred with mixed splenocytes containing 7.5×10^6 CD45.1⁺CD45.2⁺ WT TEa cells (from [TEa \times CD45.1]F1 mice) and 7.5×10^6 CD45.2⁺ *Irf4*^{-/-} TEa cells (from *Irf4*^{-/-} TEa mice) on day -1, and transplanted with BALB/c hearts on day 0. Some CD45.1⁺ recipient mice were also ip injected with 200 μ g anti-PD-L1 plus 200 μ g anti-CTLA-4 mAbs on days 0, 3, 5. TEa cells in peripheral blood and spleens of transplant recipients were analyzed on the LSRFortessa flow cytometer (Beckton Dickinson, Franklin Lakes, NJ). Fluorochrome-conjugated antibodies were purchased from BioLegend (San Diego, CA) or Thermo Fisher Scientific (Waltham, MA). Zombie Aqua Fixable Viability Kit was purchased from BioLegend. Intracellular staining method was previously described.⁸

2.7 | Statistical analysis

Data were represented as mean \pm SD and analyzed with Prism version 7.0a (GraphPad Software, San Diego, CA). The *P* values of skin graft survival were determined by the Mann-Whitney test. Other measurements were performed using unpaired Student's *t* test. Differences were considered significant when *P* < .05.

3 | RESULTS

3.1 | Ablation of IRF4 in T cells abrogates their ability to reject donor-type skin grafts in heart transplanted recipients

We have previously shown that alloreactive T cell dysfunction was achieved in *Irf4*^{f1/f1}*Cd4-Cre* mice after heart transplantation.⁸ To determine whether induced T cell dysfunction affects the survival of subsequently transplanted skin allografts, *Irf4*^{f1/f1}*Cd4-Cre* recipients were first transplanted with BALB/c hearts and then transplanted with BALB/c and C3H skin allografts 30 days later. All heart allografts were permanently accepted as previously described.⁸ Importantly, none of the heart-transplanted *Irf4*^{f1/f1}*Cd4-Cre* mice rejected the subsequently transplanted BALB/c skins (mean survival time [MST] of >100 days; n = 5) (Figure 1). By contrast, all C3H skins were rejected within 60 days (MST = 46.4 ± 10.53 days; n = 5) (Figure 1). *Irf4*^{f1/f1}*Cd4-Cre* mice without BALB/c heart transplantation were also capable of rejecting BALB/c skin grafts (MST = 31.0 ± 8.16 days; n = 4) (data not shown). Hence, ablation of IRF4 in T cells abrogated their ability to reject heart allografts and subsequently transplanted donor-type skins.

3.2 | Adoptive transfer of IRF4 re-introduced *Irf4*^{-/-} CD4⁺ T cells inhibits the induction of transplant tolerance in mice with T cell-specific IRF4 deletion

One approach that has been applied in restoring heart transplant rejection in *Irf4*^{f1/f1}*Cd4-Cre* mice was to transfer IRF4 re-introduced *Irf4*^{-/-} CD4⁺ T cells. *Irf4*^{-/-} CD4⁺ T cells were stimulated in vitro with allogenic BALB/c splenic DCs and IL-2 for 3 days, followed by transduction with IRF4-GFP or GFP-Ctrl retrovirus for 1 day. *Irf4*^{f1/f1}*Cd4-Cre* recipients injected with one million IRF4 re-introduced, but not GFP-Ctrl transduced, *Irf4*^{-/-} CD4⁺ T cells acutely rejected heart allografts within 6 days, as previously described.⁸ Recipient mice were transplanted again with skin allografts 30 days after heart grafting. As shown in Figure

2, BALB/c skins were acutely rejected on heart-transplanted recipients that were transferred with IRF4 re-introduced *Irf4*^{-/-} CD4⁺ T cells (IRF4-GFP cell transfer group; BALB/c skin; MST = 17.0 ± 6.27 days; n = 4), but were accepted on heart-transplanted recipients that were transferred with GFP-Ctrl transduced *Irf4*^{-/-} CD4⁺ T cells (GFP-Ctrl cell transfer group; BALB/c skin; MST of >100 days; n = 4) (Figure 2). C3H skins were rejected within 60 days on heart-transplanted recipients that were transferred with GFP-Ctrl transduced *Irf4*^{-/-} CD4⁺ T cells (GFP-Ctrl cell transfer group; C3H skin; MST = 45.3 ± 8.50 days; n = 4) (Figure 2). Therefore, adoptive transfer of IRF4 re-introduced, but not GFP-Ctrl transduced, *Irf4*^{-/-} CD4⁺ T cells inhibit the induction of transplant tolerance in heart-transplanted *Irf4*^{fl/fl} *Cd4-Cre* recipients.

3.3 | Immune checkpoint blockade induces heart transplant rejection but does not prevent the later establishment of transplant tolerance in mice with T cell-specific IRF4 deletion

Checkpoint blockade restored acute heart transplant rejection in *Irf4*^{fl/fl} *Cd4-Cre* mice⁸. Herein we investigated the influence of initial checkpoint blockade-mediated heart allograft rejection on the survival of subsequently transplanted skins. We transplanted BALB/c hearts into *Irf4*^{fl/fl} *Cd4-Cre* mice and treated them with anti-PD-L1 and anti-CTLA-4 mAbs on days 0, 3, and 5 post-heart grafting. All heart allografts were acutely rejected within 8 days as previously described.⁸ Recipients with rejected heart allografts were then transplanted again with skin allografts 30 days after heart grafting. Strikingly, all BALB/c skins were accepted on those recipients (MST of >100 days; n = 6), while all C3H skins were rejected within 60 days (MST = 47.0 ± 9.67 days; n = 6) (Figure 3). Therefore, checkpoint blockade induced acute heart transplant rejection in *Irf4*^{fl/fl} *Cd4-Cre* recipients, but did not prevent the later establishment of transplant tolerance.

3.4 | Identification of un-restored gene expressions in *Irf4*-deficient alloreactive T cells upon checkpoint blockade

TCR-transgenic TEa CD4⁺ T cells (B6 background) recognize a BALB/c I-Ea allopeptide presented by B6 antigen presenting cells, and were used to assess the effects of checkpoint blockade on *Irf4*-deficient alloreactive T cells.⁸ Herein, we compared the gene expression profiles between WT and *Irf4*^{-/-} TEa cells following heart transplantation and checkpoint blockade. CD45.1⁺ B6 mice were adoptively transferred with either CD45.2⁺ WT TEa or CD45.2⁺ *Irf4*^{-/-} TEa cells on day-1, and transplanted with BALB/c hearts on day 0. Recipients transferred with *Irf4*^{-/-} TEa cells were further treated with rat IgG or anti-PD-L1 plus anti-CTLA-4 mAbs (P+C group) on days 0, 3, and 5. Adoptively transferred CD45.2⁺ TEa cells were isolated from splenocytes on day 6 by flow cytometry sorting (Figure 4A). RNA was isolated and gene expression profiles were determined by microarray analysis. Differentially expressed genes between adoptively transferred WT TEa and *Irf4*^{-/-} TEa cells (IgG group) are shown in Figure 4B. Importantly, checkpoint blockade (*Irf4*^{-/-} TEa; P+C group) restored the expression levels of the majority of WT TEa cell-expressed genes in *Irf4*^{-/-} TEa cells (Figure 4B), which may explain why checkpoint blockade robustly reversed the initial dysfunction of *Irf4*^{-/-} T cells. Some of the un-restored genes in *Irf4*^{-/-} TEa cells following checkpoint blockade were shown in Figure 4C. It would be interesting

to further determine whether these unrestored genes are responsible for the reinvigorated *Irf4*-deficient T cells to become re-dysfunction.

3.5 | Checkpoint blockade does not restore effector memory cell generation from *Irf4*-deficient alloreactive T cells

To track the fate of *Irf4*^{-/-} alloreactive T cells, CD45.1⁺ B6 mice were adoptively transferred with mixed splenocytes containing a 1:1 ratio of CD45.1⁺CD45.2⁺ WT TEa (from [TEa × CD45.1]F1 mice) and CD45.2⁺ *Irf4*^{-/-} TEa cells (from *Irf4*^{-/-} TEa mice) 1 day prior to BALB/c heart transplantation (Figure 5A). TEa cell frequencies in peripheral blood were assessed weekly post-grafting. Flow cytometry plots in Figure 5B show the gating strategy detecting co-transferred CD45.1⁺CD45.2⁺TCR Vβ6⁺ WT TEa and CD45.1⁻CD45.2⁺TCR Vβ6⁺ *Irf4*^{-/-} TEa cells in peripheral blood at 1 week post-grafting. Both WT TEa and *Irf4*^{-/-} TEa cell frequencies were gradually decreased in peripheral blood (Figure 5B, line graph). On day 30 post-grafting, splenocytes of transplant recipients were harvested and analyzed. The percentage of *Irf4*^{-/-} TEa cells among CD4⁺ splenocytes was significantly lower than that of WT TEa cells (Figure S1A, i). Flow cytometry plots in Figure 5C show the gating strategy detecting TEa cell populations, and the percentages of CD62L⁻CD44⁺ effector memory and IFN-γ⁺TNF-α^{hi} cells within WT TEa (top plots) and *Irf4*^{-/-} TEa (bottom plots) cell populations, respectively. Compared to WT TEa cells, *Irf4*^{-/-} TEa cells exhibited significantly lower frequencies of effector memory and IFN-γ/TNF-α producing cells (Figure 5C, bar graphs). Percentages of IL-2⁺, PD-1⁺, and CX3CR1⁺, as well as mean fluorescence intensity (MFI) of CCR2 and CCR7 were not significantly different between WT and *Irf4*^{-/-} TEa cells in spleens when n = 3 per group (Figure S1A, ii-vi).

To track the fate of *Irf4*^{-/-} alloreactive T cells following checkpoint blockade, CD45.1⁺ B6 mice received cell transfer and heart transplantation as mentioned above, and treated with anti-PD-L1 plus anti-CTLA-4 mAbs on days 0, 3, and 5 post-grafting (Figure 5D). Both WT TEa and *Irf4*^{-/-} TEa cell frequencies remained gradually declined in peripheral blood despite of checkpoint blockade (Figure 5E). On day 30 post-grafting, the percentage of *Irf4*^{-/-} TEa cells among CD4⁺ splenocytes was significantly lower than that of WT TEa cells (Figure S1B, i). *Irf4*^{-/-} TEa cells displayed significantly lower frequencies of effector memory and IFN-γ/TNF-α producing cells than those of WT TEa cells (Figure 5F). Percentages of IL-2⁺, perforin/granzyme B⁺, PD-1⁺, and CX3CR1⁺, as well as MFI of CCR2, CCR7, TIM-3, and LAG-3 were not significantly different between WT and *Irf4*^{-/-} TEa cells in spleens when n = 3 per group (Figure S1B, ii-ix). Of note, CX3CR1 has been reported as a marker for anti-PD-1 therapy-responsive T cells,¹³ whereas CCR2 expressed on T cells has been shown to modulate the effector/regulatory T cell ratio.¹⁴ Taken together, checkpoint blockade does not restore cell frequency, effector memory cell generation, and IFN-γ/TNF-α production of *Irf4*^{-/-} TEa cells at day 30 post-grafting.

4 | DISCUSSION

Sixty-five years ago, Medawar et al demonstrated that mice injected at birth with allogeneic cells were subsequently able to accept skin allografts from the same donor strain.¹⁵ Since then transplant tolerance was further achieved in adult animals through various approaches.

^{16,17} Deletion, anergy, and Treg suppression of alloreactive T cells contribute to transplant tolerance.^{18–21} We have previously shown that ablation of IRF4 induced allogeneic T cell dysfunction.⁸ Loss of IRF4 expression has also been shown to be associated with tumor-specific T cell dysfunction.¹¹ Herein, we demonstrated that ablation of IRF4 in T cells induced robust transplant tolerance in heart allograft recipients, resulting in the acceptance of secondary donor-type skin allografts. We noticed that *Irf4^{fl/fl}Cd4-Cre* mice were capable of rejecting primary skin allografts and secondary third-party skin allografts. It is possible that heart and skin allografts exhibit different capabilities in driving the dysfunctional differentiation of *Irf4*-deficient T cells.

Checkpoint blockade induced acute heart transplant rejection in *Irf4^{fl/fl}Cd4-Cre* recipients.⁸ Our previous mechanistic studies revealed that checkpoint blockade restored cell number, proliferation (indicated by Ki67), metabolic activation (indicated by CD98 and CD71), and IFN- γ production of *Irf4^{-/-}* TEa cells on day 6 post-heart grafting.⁸ In this study, we compared the gene expression profiles between WT TEa and *Irf4^{-/-}* TEa cells in heart recipients on day 6, and found that checkpoint blockade also restored many other genes in *Irf4^{-/-}* TEa cells, including *Tbx21*, *Il12rb1*, *Il2rb*, *Il2rg*, *Il10rb*, *Il15ra*, and *Il21r* (data not shown). Hence, restoring some cytokine responses may be another essential mechanism by which checkpoint blockade transiently reinvigorates *Irf4^{-/-}* T cells. Nevertheless, checkpoint blockade did not prevent the later establishment of transplant tolerance. Hence, similar to the re-exhaustion of reinvigorated T cells in a chronic infection model,²² reinvigorated *Irf4*-deficient T cells also became re-dysfunctional in our model. We identified un-restored gene expressions in *Irf4^{-/-}* TEa cells upon checkpoint blockade. For instance, regardless with or without checkpoint blockade, *Irf4^{-/-}* TEa cells exhibited down-regulated expressions of *Il18r1* (encoding IL-18R α) and *Wnt10a*, as well as up-regulated expression of *Il1r2* (encoding IL-1R2). IL-18R α has been shown to be down-regulated on exhausted CD8⁺ T Cells, rendering them unresponsive to inflammatory cytokines.²³ IL-1R2 is a negative regulator of IL-1 signaling,²⁴ whereas Wnt signaling is essential for T cell memory.²⁵ It remains to be determined the role of these un-restored genes in establishing the irreversible state of *Irf4^{-/-}* T cell dysfunction.

It is a challenge to determine whether transplant tolerance has been achieved in the clinic, and how to proceed if it has not. Successful weaning from immunosuppression may be an indication of transplant tolerance, but it remains unclear how to stratify transplant recipients according to their likelihood of being able to discontinue immunosuppression. Moreover, transplant tolerance can be achieved and maintained after rejection, as demonstrated in murine and larger animal models.^{26–30} Hence, there is a fundamental need to reveal the determinants of T cell fate in transplant tolerance. The current works identified IRF4 as a key determinant governing transplant tolerance, which will advance the understanding and further characterization of tolerogenic T cell fate.

Supplementary Material

Refer to Web version on PubMed Central for supplementary material.

ACKNOWLEDGMENTS

This study was supported by the startup fund from Houston Methodist Research Institute (to W.C.) and the US National Institutes of Health grant (#NIH R01AI132492 to W.C.). The authors thank the Flow Cytometry Core at Houston Methodist and the Genomic and RNA Profiling Core at Baylor College of Medicine for excellent services.

Funding information

Houston Methodist Research Institute; National Institute of Allergy and Infectious Diseases, Grant/Award Number: R01AI132492

Abbreviations:

B6	C57BL/6
CTLA-4	cytotoxic T-lymphocyte-associated protein 4
Ctrl	control
DCs	dendritic cells
HTx	heart transplantation
IRF4	interferon regulatory factor 4
MST	mean survival time
PD-1	programmed cell death protein 1
PD-L1	programmed death-ligand 1
TCR	T cell receptor
Tx	transplantation
WT	wild-type

REFERENCES

1. Sawinski D, Trofe-Clark J, Leas B, et al. Calcineurin inhibitor minimization, conversion, withdrawal, and avoidance strategies in renal transplantation: a systematic review and meta-analysis. *Am J Transplant.* 2016;16(7):2117–2138. [PubMed: 26990455]
2. Li XC, Rothstein DM, Sayegh MH. Costimulatory pathways in transplantation: challenges and new developments. *Immunol Rev.* 2009;229(1):271–293. [PubMed: 19426228]
3. Miyahara Y, Khattar M, Schroder PM, et al. Anti-TCRbeta mAb induces long-term allograft survival by reducing antigen-reactive T cells and sparing regulatory T cells. *Am J Transplant.* 2012;12(6):1409–1418. [PubMed: 22420295]
4. Chen W, Ghobrial RM, Li XC. The evolving roles of memory immune cells in transplantation. *Transplantation.* 2015;99(10):2029–2037. [PubMed: 26102615]
5. Ochiai K, Maienschein-Cline M, Simonetti G, et al. Transcriptional regulation of germinal center B and plasma cell fates by dynamical control of IRF4. *Immunity.* 2013;38(5):918–929. [PubMed: 23684984]
6. Huber M, Lohoff M. IRF4 at the crossroads of effector T-cell fate decision. *Eur J Immunol.* 2014;44(7):1886–1895. [PubMed: 24782159]

7. Vander Lugt B, Khan AA, Hackney JA, et al. Transcriptional programming of dendritic cells for enhanced MHC class II antigen presentation. *Nat Immunol.* 2014;15(2):161–167. [PubMed: 24362890]
8. Wu J, Zhang H, Shi X, et al. Ablation of transcription factor IRF4 promotes transplant acceptance by driving allogeneic CD4(+) T cell dysfunction. *Immunity.* 2017;47(6):1114–1128 e6. [PubMed: 29221730]
9. Alhamad T, Venkatachalam K, Linette GP, Brennan DC. Checkpoint inhibitors in kidney transplant recipients and the potential risk of rejection. *Am J Transplant.* 2016;16(4):1332–1333. [PubMed: 26752406]
10. Lipson EJ, Bagnasco SM, Moore J, et al. Tumor regression and allograft rejection after administration of anti-PD-1. *N Engl J Med.* 2016;374(9):896–898.
11. Philip M, Fairchild L, Sun L, et al. Chromatin states define tumour-specific T cell dysfunction and reprogramming. *Nature.* 2017;545(7655):452–456. [PubMed: 28514453]
12. Garrod KR, Cahalan MD. Murine skin transplantation. *J Vis Exp.* 2008;11:e634.
13. Yan Y, Cao S, Liu X, et al. CX3CR1 identifies PD-1 therapy-responsive CD8 + T cells that withstand chemotherapy during cancer chemoimmunotherapy. *JCI Insight.* 2018;3(8):e97828.
14. Bakos E, Thaïss CA, Kramer MP, et al. CCR2 regulates the immune response by modulating the interconversion and function of effector and regulatory T cells. *J Immunol.* 2017;198(12):4659–4671. [PubMed: 28507030]
15. Billingham RE, Brent L, Medawar PB. Actively acquired tolerance of foreign cells. *Nature.* 1953;172(4379):603–606. [PubMed: 13099277]
16. Larsen CP, Elwood ET, Alexander DZ, et al. Long-term acceptance of skin and cardiac allografts after blocking CD40 and CD28 pathways. *Nature.* 1996;381(6581):434–438. [PubMed: 8632801]
17. Wekerle T, Kurtz J, Ito H, et al. Allogeneic bone marrow transplantation with co-stimulatory blockade induces macrochimerism and tolerance without cytoreductive host treatment. *Nat Med.* 2000;6(4):464–469. [PubMed: 10742157]
18. Monk NJ, Hargreaves RE, Marsh JE, et al. Fc-dependent depletion of activated T cells occurs through CD40L-specific antibody rather than costimulation blockade. *Nat Med.* 2003;9(10):1275–1280. [PubMed: 14502279]
19. Daley SR, Cobbold SP, Waldmann H. Fc-disabled anti-mouse CD40L antibodies retain efficacy in promoting transplantation tolerance. *Am J Transplant.* 2008;8(11):2265–2271. [PubMed: 18782294]
20. Taylor PA, Noelle RJ, Blazar BR. CD4(+)CD25(+) immune regulatory cells are required for induction of tolerance to alloantigen via costimulatory blockade. *J Exp Med.* 2001;193(11):1311–1318. [PubMed: 11390438]
21. Zuber J, Sykes M. Mechanisms of mixed chimerism-based transplant tolerance. *Trends Immunol.* 2017;38(11):829–843. [PubMed: 28826941]
22. Pauken KE, Sammons MA, Odorizzi PM, et al. Epigenetic stability of exhausted T cells limits durability of reinvigoration by PD-1 blockade. *Science.* 2016;354(6316):1160–1165. [PubMed: 27789795]
23. Ingram JT, Yi JS, Zajac AJ. Exhausted CD8 T cells downregulate the IL-18 receptor and become unresponsive to inflammatory cytokines and bacterial co-infections. *PLoS Pathog.* 2011;7(9):e1002273. [PubMed: 21980291]
24. Peters VA, Joesting JJ, Freund GG. IL-1 receptor 2 (IL-1R2) and its role in immune regulation. *Brain Behav Immun.* 2013;32:1–8. [PubMed: 23195532]
25. Gattinoni L, Zhong XS, Palmer DC, et al. Wnt signaling arrests effector T cell differentiation and generates CD8 + memory stem cells. *Nat Med.* 2009;15(7):808–813. [PubMed: 19525962]
26. Miller ML, Alegre ML, Chong AS. Transplantation tolerance after allograft rejection. *Curr Opin Organ Transplant.* 2017;22(1):64–70. [PubMed: 27898463]
27. Yamada Y, Nadazdin O, Boskovic S, et al. Repeated injections of IL-2 break renal allograft tolerance induced via mixed hematopoietic chimerism in monkeys. *Am J Transplant.* 2015;15(12):3055–3066. [PubMed: 26190648]

28. Scalea JR, Okumi M, Villani V, et al. Abrogation of renal allograft tolerance in MGH miniature swine: the role of intra-graft and peripheral factors in long-term tolerance. *Am J Transplant.* 2014;14(9):2001–2010. [PubMed: 25100613]
29. Young JS, Daniels MD, Miller ML, et al. Erosion of transplantation tolerance after infection. *Am J Transplant.* 2017;17(1):81–90. [PubMed: 27273890]
30. Miller ML, Daniels MD, Wang T, et al. Spontaneous restoration of transplantation tolerance after acute rejection. *Nat Commun.* 2015;6:7566. [PubMed: 26151823]

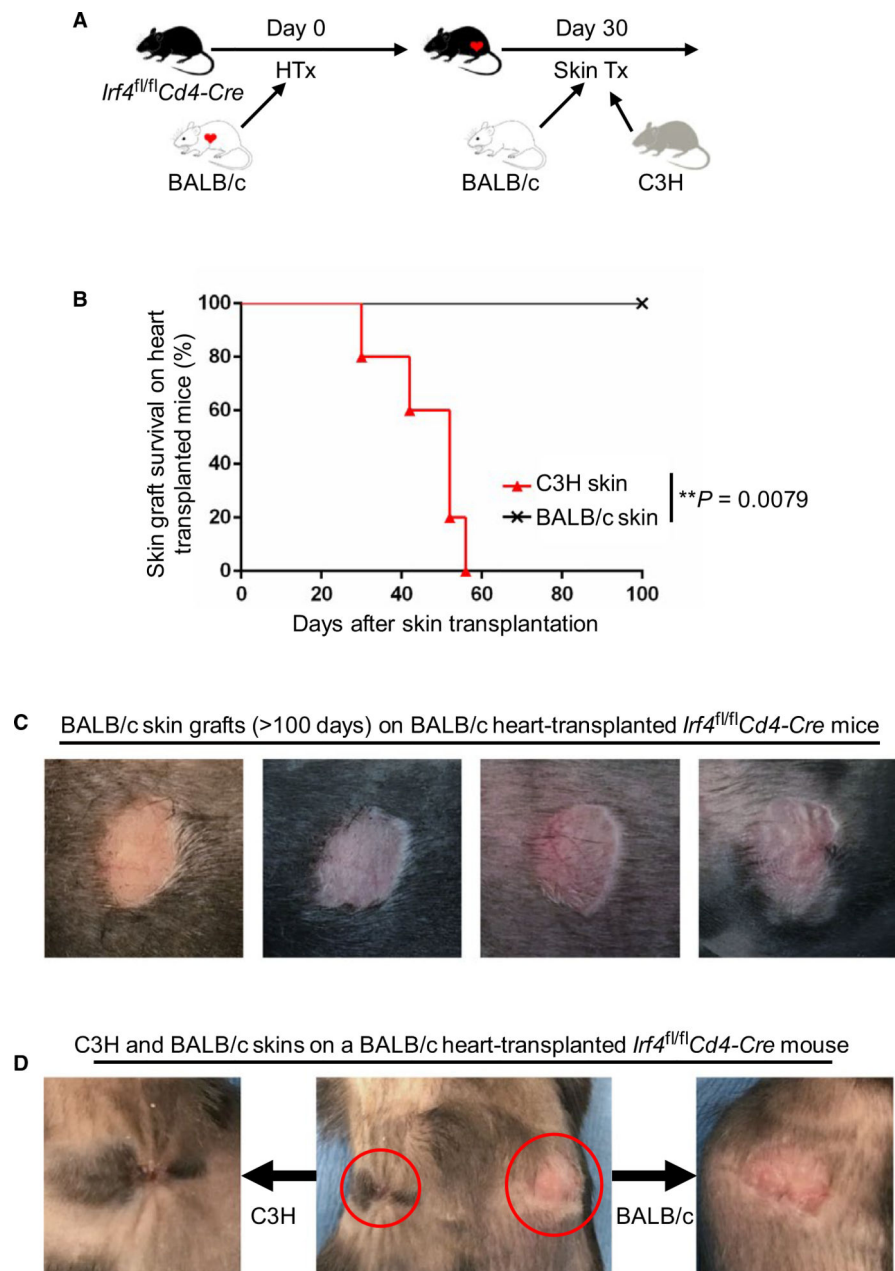


FIGURE 1. IRF4 deletion in T cells induces transplant tolerance in heart graft recipients. *Irif4^{fl/fl}Cd4-Cre* mice were transplanted with BALB/c hearts. Thirty days later, recipients were transplanted again with BALB/c and C3H skins (n = 5). A, Schematic of the experimental design. B, The percentage of skin allograft survival after skin transplantation on BALB/c heart-transplanted *Irif4^{fl/fl}Cd4-Cre* recipients. ***P* = .0079; Mann-Whitney test. C, Representative images of accepted BALB/c skin allografts (>100 days) on BALB/c heart-transplanted *Irif4^{fl/fl}Cd4-Cre* recipients. D, A representative image of C3H (left) and BALB/c (right) skin allografts on a BALB/c heart-transplanted *Irif4^{fl/fl}Cd4-Cre* recipient

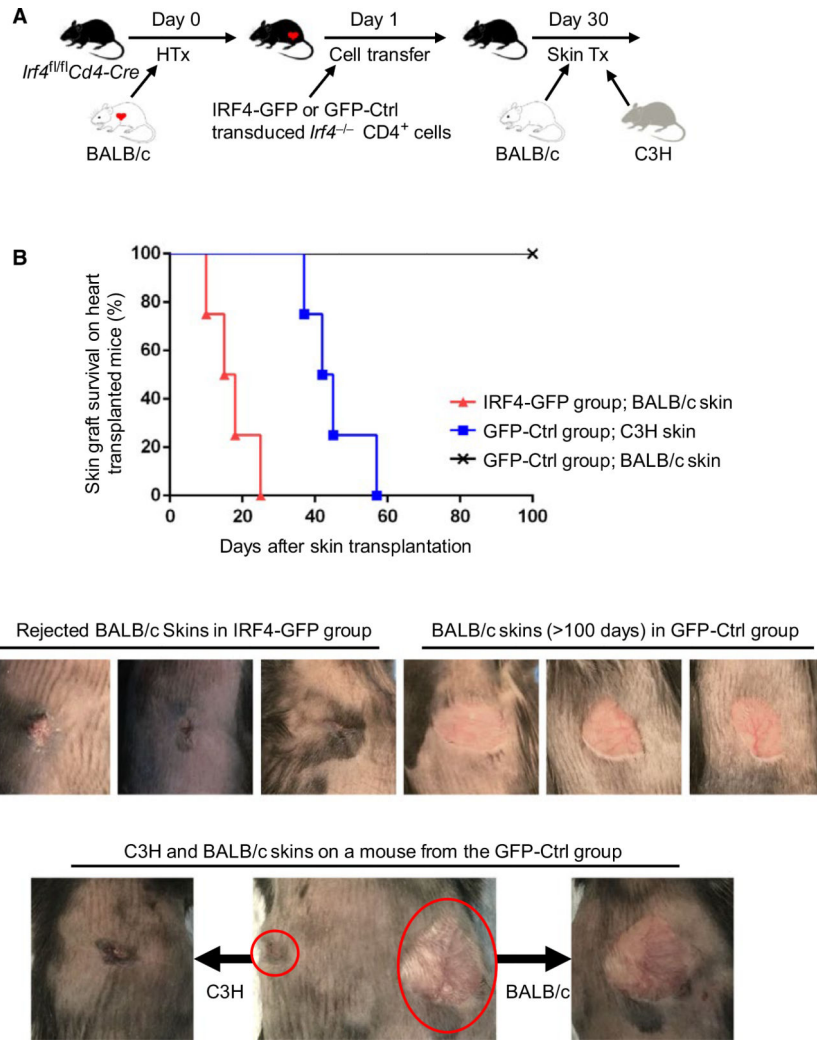
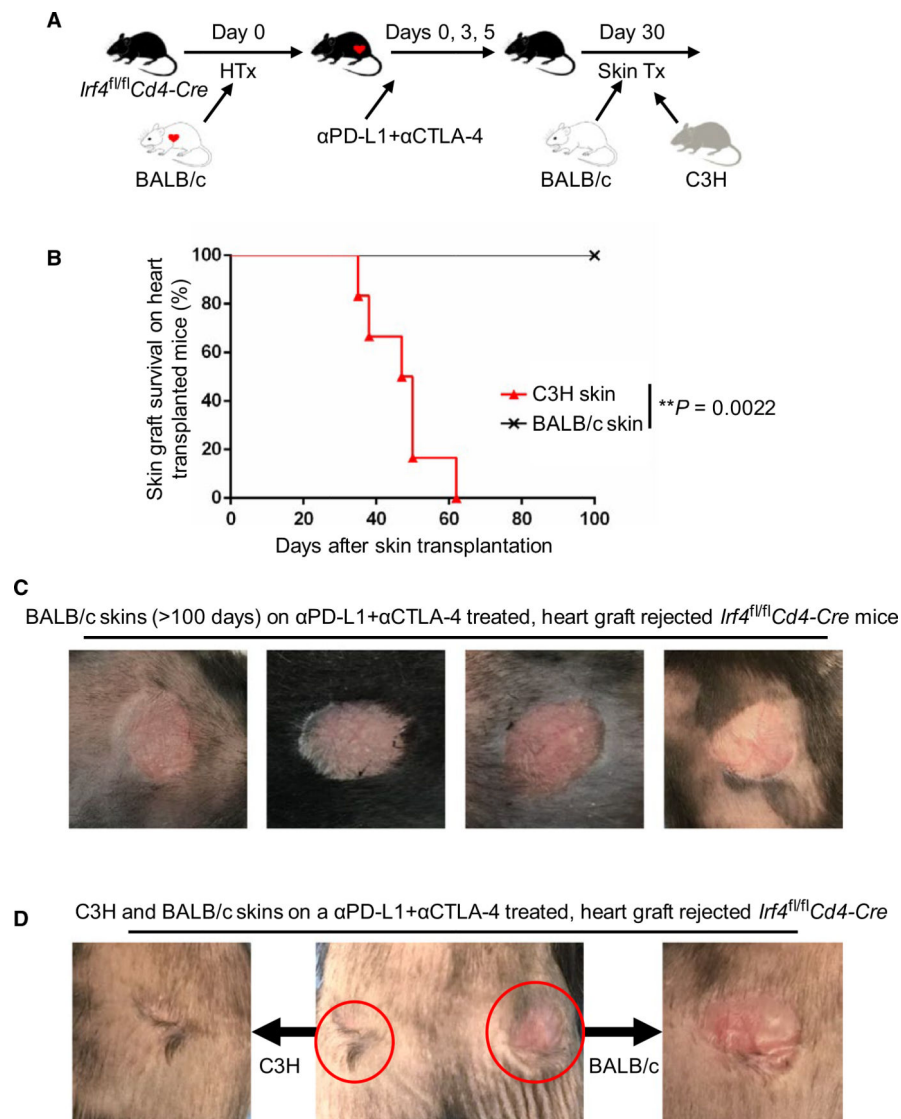
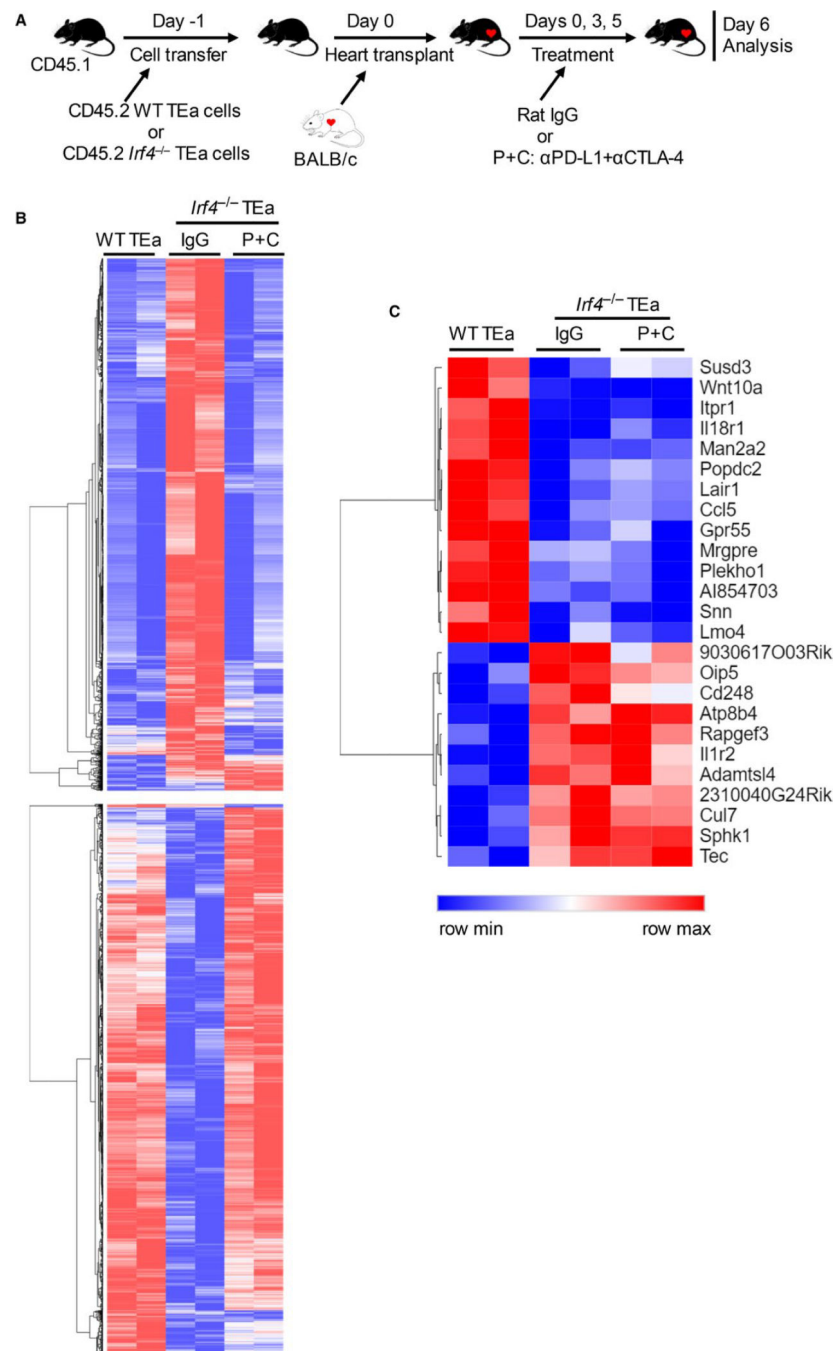


FIGURE 2. Adoptive transfer of IRF4 re-introduced *Irf4^{-/-} CD4⁺* T cells breaks transplant tolerance in *Irf4*-deficient mice. *Irf4^{-/-} CD4⁺* T cells were stimulated with allogenic BALB/c splenic DCs and IL-2 for 3 days, followed by transduction with IRF4-GFP or GFP-Ctrl retrovirus for 1 day. *Irf4^{fl/fl}Cd4-Cre* mice were transplanted with BALB/c hearts on day 0 and adoptively transferred with one million IRF4-GFP or GFP-Ctrl transduced *Irf4^{-/-} CD4⁺* T cells on day 1. Thirty days later, recipient mice in the IRF4-GFP group were transplanted again with BALB/c skins (n = 4), whereas recipients in the GFP-Ctrl group were transplanted with both C3H and BALB/c skins (n = 4). A, Schematic of the experimental design. B, The percentage of skin allograft survival after skin transplantation on BALB/c heart-transplanted *Irf4^{fl/fl}Cd4-Cre* recipients that had been adoptively transferred with IRF4-GFP or GFP-Ctrl transduced *Irf4^{-/-} CD4⁺* T cells. C, Representative images of rejected (left 3 panels) and accepted (right 3 panels) BALB/c skins on BALB/c heart transplanted *Irf4^{fl/fl}Cd4-Cre* recipients that had been adoptively transferred with IRF4-GFP and GFP-Ctrl transduced *Irf4^{-/-} CD4⁺* T cells, respectively. D, A representative image of C3H (left) and BALB/c (right) skin allografts on a BALB/c heart-transplanted *Irf4^{fl/fl}Cd4-Cre* mouse that had been adoptively transferred with GFP-Ctrl transduced *Irf4^{-/-} CD4⁺* T cells

**FIGURE 3.**

Checkpoint blockade does not prevent the establishment of transplant tolerance in *Irf4*-deficient mice. *Irf4^{fl/fl}Cd4-Cre* mice were transplanted with BALB/c hearts on day 0 and treated with anti-PD-L1 and anti-CTLA-4 (αPD-L1 + αCTLA-4) mAbs on days 0, 3, and 5 to trigger heart graft rejection. Recipients with rejected heart allografts were then transplanted again with BALB/c and C3H skin allografts 30 days after heart grafting (n = 6). A, Schematic of the experimental design. B, The percentage of skin allograft survival after skin transplantation on αPD-L1 + αCTLA-4 treated, BALB/c heart graft rejected *Irf4^{fl/fl}Cd4-Cre* mice. ***P* = .0022; Mann-Whitney test. C, Representative images of accepted BALB/c skin allografts (>100 days) on αPD-L1 + αCTLA-4 treated, BALB/c heart graft rejected *Irf4^{fl/fl}Cd4-Cre* recipients. D, A representative image of C3H (left) and BALB/c (right) skin allografts on a αPD-L1 + αCTLA-4 treated, BALB/c heart graft rejected *Irf4^{fl/fl}Cd4-Cre* mouse

**FIGURE 4.**

Identification of un-restored genes in alloreactive *Irf4*^{-/-} CD4⁺ T cells upon checkpoint blockade. CD45.1⁺ B6 mice were adoptively transferred with CD45.2⁺ WT or *Irf4*^{-/-} TEa cells on day -1, and transplanted with BALB/c hearts on day 0. Recipients transferred with *Irf4*^{-/-} TEa cells were further treated with rat IgG or anti-PD-L1 plus anti-CTLA-4 mAbs (P+C group) on days 0, 3, and 5. Adoptively transferred CD45.2⁺ TEa cells were isolated from splenocytes on day 6 by flow cytometry sorting. RNA was isolated for microarray analysis. A, Schematic of the experimental design. B and C, Heat maps showing the normalized gene

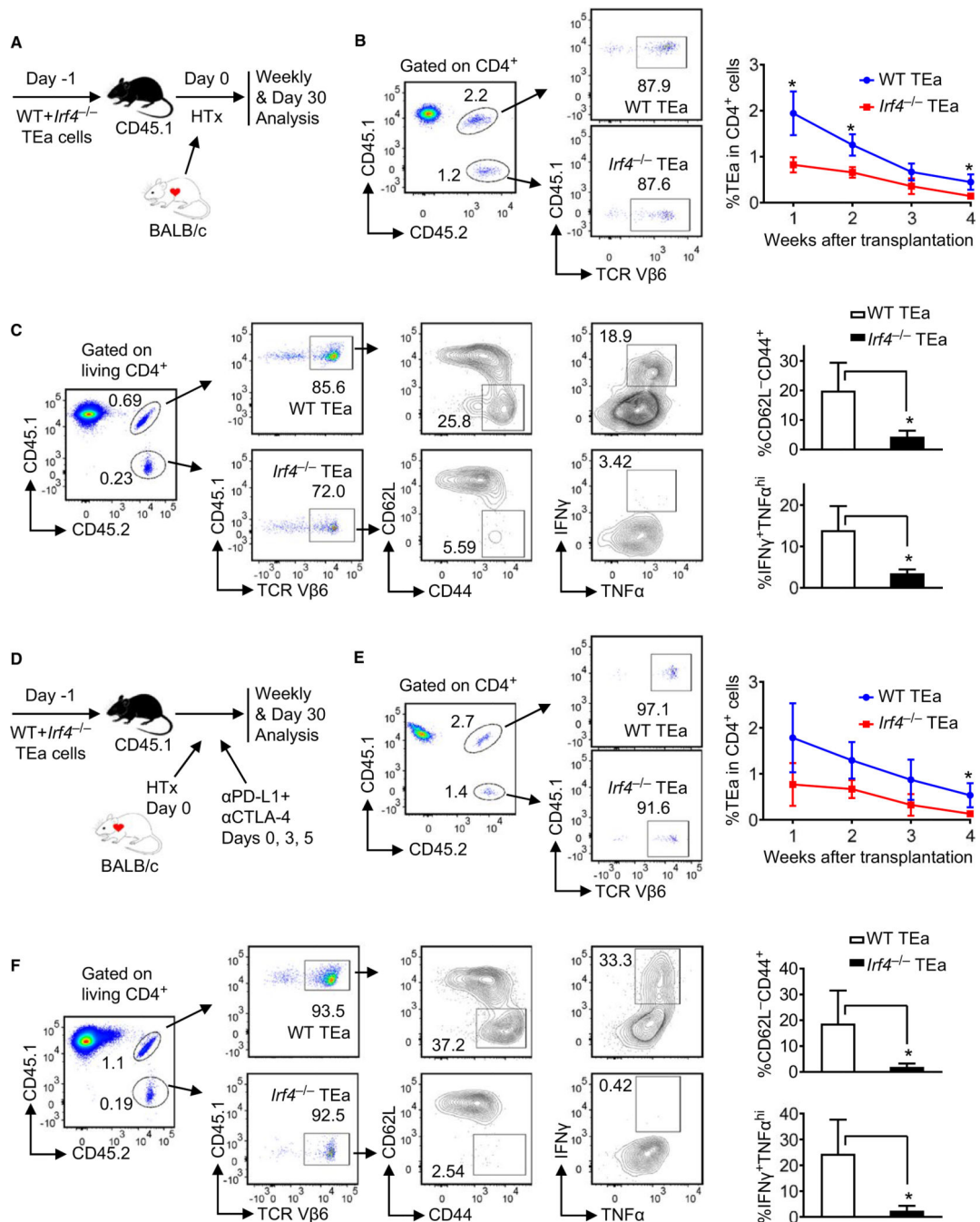
expression scores from indicated groups. Two RNA samples of each group were obtained from two independent experiments. Each RNA sample was isolated from pooled TEa cells from three (WT TEa group and *Irf4*^{-/-} TEa P+C group) or five (*Irf4*^{-/-} TEa IgG group) recipient mice

Author Manuscript

Author Manuscript

Author Manuscript

Author Manuscript

**FIGURE 5.**

Checkpoint blockade does not restore effector memory cell generation from alloreactive *Irf4*^{-/-} CD4⁺ T cells. CD45.1⁺ B6 mice were adoptively transferred with mixed splenocytes containing a 1:1 ratio of CD45.1⁺CD45.2⁺ WT TEa and CD45.2⁺ *Irf4*^{-/-} TEa cells on day -1, transplanted with BALB/c hearts on day 0, and left untreated (A-C) or treated with αPD-L1 + αCTLA-4 (D-F) on days 0, 3, and 5. A, Schematic of the experimental design. B, Flow cytometry plots display the gating strategy detecting co-transferred CD45.1⁺CD45.2⁺TCR Vβ6⁺ WT TEa and CD45.1⁻CD45.2⁺TCR Vβ6⁺ *Irf4*^{-/-} TEa cells in peripheral blood at 1

week post-grafting. The line graph shows WT TEa and *Irf4*^{-/-} TEa cell frequencies in peripheral blood weekly after transplantation. C, Splenocytes were analyzed on day 30 post-grafting. Shown are the gating strategy detecting TEa cell populations, and the percentages of CD62L⁻CD44⁺ and IFN- γ ⁺TNF- α ^{hi} cells within WT TEa and *Irf4*^{-/-} TEa cell populations. D, Schematic of the experimental design, with α PD-L1 + α CTLA-4 treatment. E, WT TEa and *Irf4*^{-/-} TEa cell frequencies in peripheral blood at 1 week post-grafting (flow cytometry plots) and weekly after transplantation (line graph). F, The percentages of CD62L⁻CD44⁺ and IFN- γ ⁺TNF- α ^{hi} cells within WT TEa and *Irf4*^{-/-} TEa cells in spleens at day 30 post-grafting. Data are mean \pm SD (n = 3). **P* < .05